American Mineralogist, Volume 81, pages 1452–1459, 1996

A reevaluation of crystal-size distributions in chromite cumulates

C. Waters and A.E. Boudreau

Department of Geology, Duke University, Box 90227, Durham, North Carolina 27708, U.S.A.

Abstract

Although studies have shown that igneous cumulates can form by in situ crystallization without requiring crystal settling, it has not been demonstrated that crystal-size distributions (CSDs) are consistent with such a process. Plots of crystal-size fractions per unit volume vs. crystal size for chromite grains from the Stillwater complex show a log-linear distribution with negative slope at larger sizes and a concave-down distribution at smaller sizes. The log-linear portion of these trends is similar to previously reported trends for other silicate and oxide phases in crystallizing magmas. However, the lack of smaller grain sizes indicates that the original population was altered during a postnucleation crystal-aging period that resulted in the loss of the smaller size fractions, an interpretation consistent with textural and volume-balance evidence. The CSD trends imply that Cr was not concentrated by settling of chromite but was brought to the site of the growing chromite grains. Similarities between the Stillwater data and CSD trends for garnet in metapelites suggest that such trends are a characteristic feature of any geologic system undergoing crystal aging after an initial period of nucleation and crystal growth.

Introduction

Textural studies of igneous rocks are important because grain size, shape, and distribution contain information about magma crystallization. Most existing studies of crystal-size distributions (CSDs) of cumulus minerals in layered intrusions have been largely concerned with comparisons with size distributions produced by sedimentary processes, and interpretations have concentrated on the hydraulic properties of crystals as described by their size and density. For example, in the classic study of chromite and olivine cumulates from the Ultramafic series of the Stillwater Complex of Montana, Jackson (1961) noted that these minerals display size-frequency curves similar to those observed in sedimentary rocks. Although this evidence supported crystal deposition by settling, the crystal densities of all the cumulus phases present within a rock did not necessarily display hydraulic equivalency nor were they generally accompanied by a graded density-radius distribution as is typical for sandstone. Because of this, Jackson was among the first to suggest that crystal settling may not have been the dominant mechanism of crystal accumulation and that, in most instances, the cumulus phases grew in situ at the bottom of the magma chamber. This interpretation was further developed by the work of Campbell (1978) and McBirney and Noyes (1979). However, none of these studies demonstrated that CSD plots for cumulus minerals are consistent with in situ nucleation and growth processes.

As summarized by Marsh (1988), CSD data are most amenable to forward modeling when grain-size data are plotted as ln n_L vs. L, where n_L is the number of grains per unit volume of size class L. In many instances of igneous crystallization (such as lava lakes), minerals as diverse as plagioclase and iron titanium oxides display a log-linear trend with a negative slope when plotted in this manner (Cashman and Marsh 1988). A log-linear trend can result from one of several physical mechanisms. For example, it can occur when the nucleation rate, n_0, and growth rate, G, are both constant with time, but when crystals have an average residence time, τ. The simplest equations describing this relationship are similar to radioactive decay equations, in which L/G is analogous to time and $1/\tau$ is equivalent to the decay constant of a radioactive element. In other words, longer growth time results in greater crystal size but also increases the probability that the crystal will leave the system. A second physical interpretation of a log-linear trend is that crystals do not physically leave the system, but rather the increase in the number density of smaller sizes results from an exponentially increasing nucleation rate with time (Marsh 1988; Marsh and Ramini 1995). In this case, τ is the age of a typical crystal. Additional information on the rock's history may be needed to distinguish between these two possibilities for any given sample.

Mechanisms that can cause nonlinear trends include a preferential accumulation or loss of larger grains; the former would be expected if accumulation of larger grains resulted from crystal settling. Preferential growth of larger grains can also occur during crystal aging of a mineral assemblage as larger grains grow at the expense of energetically less-favored smaller grains (Ostwald 1900).

This study examines CSDs in a chromite cumulate from the Stillwater Complex in light of these new studies on the evolution of CSDs in crystallizing systems. It is

0003-004X/96/1112-1452$05.00

shown that CSD trends are indeed consistent with in situ nucleation processes and need not involve crystal settling.

Petrography

The sample used in this study is from a previously unreported chromitite from the upper part of Gabbronorite Zone I of the Stillwater Complex [see McCallum et al. (1980) and Raedeke and McCallum (1984) for a description of the stratigraphic subdivisions of the Stillwater Complex]. This part of the stratigraphy contrasts with the relatively uniform rocks beneath in that modal layering is common and locally shows deformation features (cf. Todd et al. 1982). The chromitite occurs as one, or locally two, deformed layers, 0.5–5 cm thick, present in broken outcrop exposed for no more than 5 m along strike; its total lateral extent is unknown. Modal abundance of chromite within the chromitite varies from 30 to 70%. Other minerals present are mainly plagioclase and pyroxene. Grain sizes are not uniformly distributed throughout a layer. In the thin layer shown in Figure 1, larger grains are noticeably concentrated in the center of the layer, whereas smaller grains are preferentially concentrated at the lower and upper margins. Outside the chromitite layers, chromite grains are generally rare and considerably smaller than those within the layers.

Methods

Grain measurements were performed on both reflected light photomicrograph mosaics and on backscattered electron-image mosaics taken with an electron microprobe. In clusters and larger groups, the grains locally impinge on each other. In some instances it is difficult to distinguish grain boundaries even with a microscope. In these cases the grain boundaries were assumed to be at the simplest interface between grains. Grains in clusters are typically of intermediate to larger size, so errors in grain-boundary placement predominantly affect the larger sizes. In addition, some grains have what appear to be residual boundaries in their interiors, as might be found in a grain that grew from the coalescence of several mutually impinging grains. Hunter (1986) suggested that this situation is the result of grain-boundary migration, whereby two of more impinging crystals become a single grain during textural equilibration. This was assumed to be the case, and these were considered to be single grains.

Crystal size was determined in one of three ways: (1) Measurements were made of the average of the longest dimension and the maximum length normal to the long axis. (2) Grain margins of sample E were digitized using a digitizing tablet, and grain size was determined from the feret diameter (diameter of a circle having the same area as the grain). (3) On sample F, grain size was determined using a particle-analysis program. Results are similar for all methods.

The problem of extracting true CSDs from measurements made on random planar sections was discussed by Cashman and Marsh (1988), whose methodology we follow here. The number of crystals per size interval, L, per unit area, n_A (crystals/cm^3), was calculated by counting the number of crystals of the given size range and dividing this number by the total area. The number per unit area was then raised to the $\frac{3}{2}$ power to get the number of crystals per unit volume, n_L (crystals/cm^4). Although n_L can be calculated directly by this method, a more stable procedure first calculates the cumulative number density, N_L:

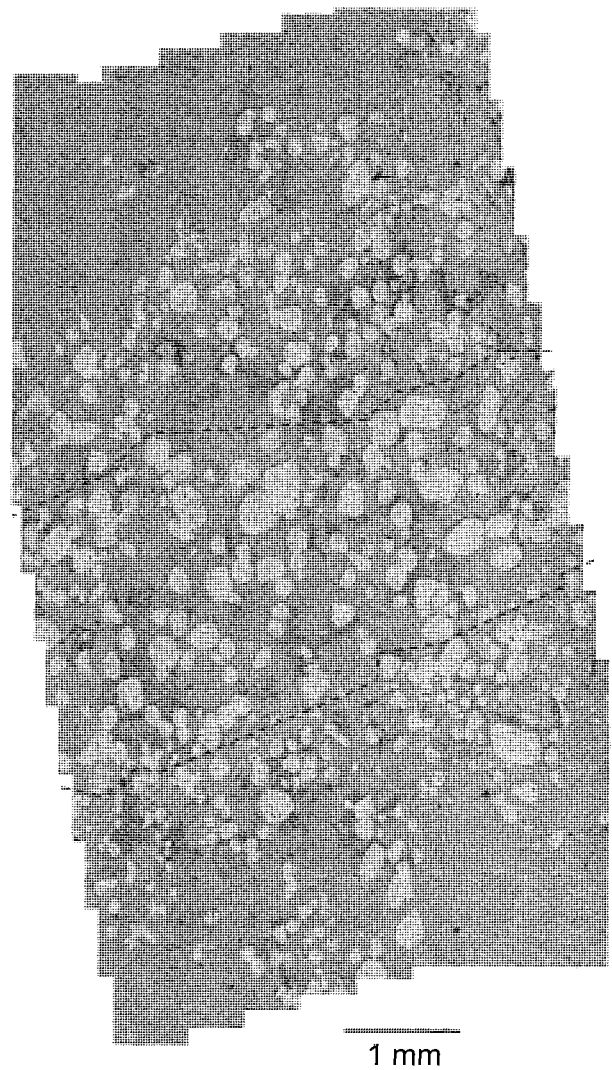

Figure 1. Photomosaic of digital backscattered electron images of a thin, symmetrically size-graded chromitite layer (sample F) from Gabbronorite Zone I of the Lower Banded series of the Stillwater Complex, Montana. Chromite grains are shown as light-colored, equant grains. Undifferentiated silicate minerals (mainly plagioclase and pyroxene) compose the darker gray background. The layer generally extends from lower left to upper right. Dashed lines outline the central region of larger grains: CSD curves were determined on all grains in the layer and on grains in the central and marginal portions separately (Fig. 4).

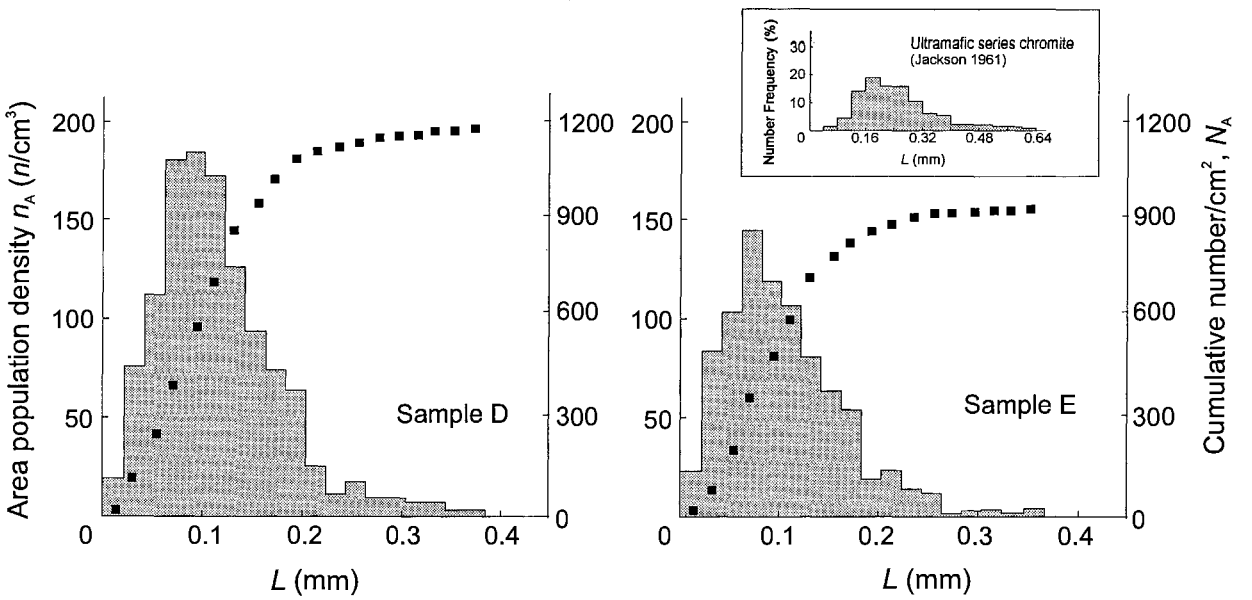

FIGURE 2. Size-frequency histograms of the number of grains of a given size interval, n_A (shaded), and cumulative frequency, N_A (squares), for samples D and E. For comparison, inset shows a typical size-frequency histogram of chromitite from the Ultramafic series (after Jackson 1961).

$$N_L = \int_0^L n_L \, dL. \quad (1)$$

The slope of the cumulative number-density curve then describes the population density, n_L, for any arbitrary width of the size interval, ΔL (e.g., Marsh 1988); n_L was calculated by numerical differentiation of the slope of the cumulative number-density curve:

$$n_L = \frac{dN_L}{dL} \approx \frac{\Delta N_L}{\Delta L}. \quad (2)$$

Finally, it was observed that the number of grains within a sample affected the amount of scatter within the distribution plots. Samples in which >1000 grains were measured produced smoother trends. The maximum number of grains counted on any one sample was 1777.

RESULTS

Figure 2 shows representative measured two-dimensional size-frequency histograms, n_A, and two-dimensional cumulative number density, N_A, for two samples, D and E, with high total grain counts. These are plots of the raw data normalized only to the area of the thin section examined for comparison with previous studies. The size distributions are characterized by bell-shaped histograms with notable tails in the larger size fractions. The corresponding cumulative number-density plots show a steep initial rise then flattening at the larger sizes. The trends in both the frequency histograms and cumulative plots are enhanced when converted to numbers of crystals per unit volume, as discussed above. The trends observed in these plots are similar to those measured by Jackson (1961) for both chromite and olivine in the Ultramafic series of the Stillwater Complex (Fig. 2, inset).

Plots of ln n_L vs. L are shown in Figure 3 for samples D and E and in Figure 4 for sample F. These plots show low number densities for the smaller sizes, a peak at intermediate sizes, and a log-linear trend for larger sizes. A least-squares fit to the linear leg of the data for each sample yielded the slope, y intercept, and r^2 regression fit noted in the plots.

Figure 4 shows the CSD trends of the symmetrically size-graded layer shown in Figure 1. Plotted are the CSD for the entire layer and the CSD for the central and marginal parts of the layer. All three CSD curves show the log-linear trend at larger sizes with a drop-off at smaller size fractions. A comparison of the linear fits illustrates that the coarser, central section forms a flatter trend than the layer as a whole, whereas the marginal grains form a steeper trend, with the trend lines rotating about a pivot point at L = 0.1 mm, ln n_L = 12.5.

DISCUSSION

The CSD trends do not show the expected flattening at larger sizes if the rocks formed by crystal settling (Marsh 1988). Instead, the log-linear portions of the curve suggests that nucleation and growth of chromite in a large, slowly cooled intrusion such as the Stillwater Complex is similar to the nucleation and growth behavior of other igneous minerals in more quickly cooled igneous environments. Following Cashman and Ferry (1988), the linear trend line can be interpreted to be at (or very close to) the CSD after nucleation ended. Thus, the slope is equal to $-1/G\tau$, and the extrapolated y intercept gives the

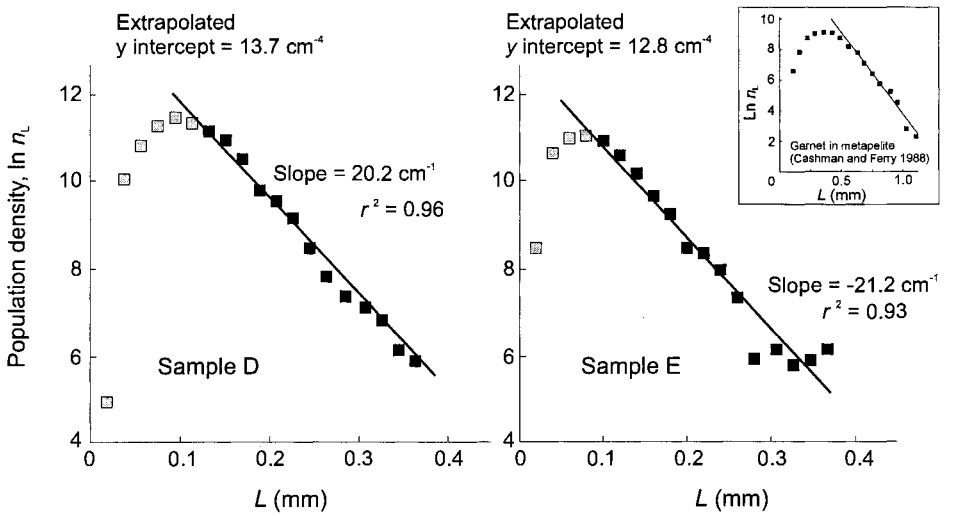

FIGURE 3. Plots of natural log of the number of crystals per given size interval per cubic centimeter, ln n_L, vs. grain size, L, for samples D and E. Least-squares regression fits for the log-linear portion of the curve were calculated for the black squares only. Inset shows similar plot for garnet in a metapelite reported by Cashman and Ferry (1988).

final nucleation density, n_0. For example, assuming that chromite grew at a rate, G, no faster than that observed for magnetite in lava lakes, 2.9×10^{-10} cm/s (Cashman and Marsh 1988), one can calculate the average residence time (or typical crystal age), τ. For sample D, $\tau = 1.71 \times 10^8$ s or 5.5 yr.

The important modification in the CSD trend appears at smaller grain sizes, where loss is consistent with the textural evidence noted above for grain-boundary migration and by Boudreau (1995) for significant chromite growth by aging. Indeed, another, natural analog to the Stillwater chromitite is in the CSD plots of minerals in metamorphosed pelites (Fig. 3, inset). Cashman and Ferry (1988) interpreted the log-linear portion of the garnet CSD trend to be the result of an initial period of nucleation and growth, with the nucleation rate increasing exponentially with time. A later period of postnucleation crystal aging resulted in the loss of the less stable, smaller crystals.

We interpret the Stillwater chromite CSD trends to have resulted from an identical process of early nucleation and growth of chromite followed by a later period of crystal aging that resulted in loss of the smaller size fraction. The trends of the Stillwater data were predicted by Cashman (1990), who suggested that such trends should be typical of CSDs developed in slowly cooled plutonic environments. The trends suggest that the phenomena of nucleation, growth, and (given enough time) crystal aging produce comparable CSD curves for many minerals in a wide variety of igneous and metamorphic environments.

CSDs that have evolved by a static aging mechanism are expected to have a unique normalized grain-size distribution that is a function of the growth law for the mineral. Theoretical crystal-aging CSD curves were origi-

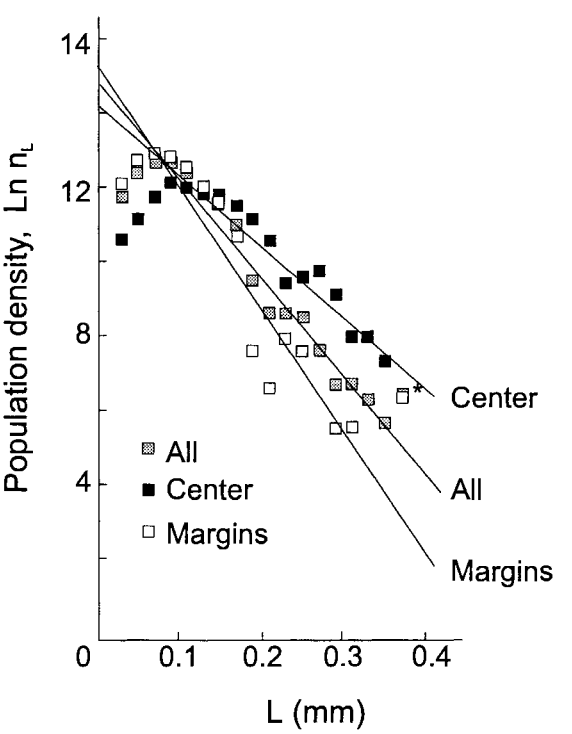

FIGURE 4. CSD plots of symmetrically size-graded layer shown in Figure 1 (sample F). Data were plotted for all grains in the layer, those in the central one-third of the layer, and those in the marginal two-thirds of the layer, as outlined in Figure 1. Linear trends were calculated for all grains equal to or larger than the most frequent, except for the one point in the marginal set marked with an asterisk, which resulted from the presence of a single large grain.

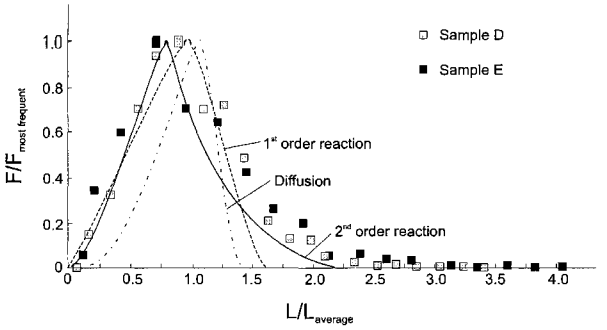

FIGURE 5. Expected grain-size distribution curves for spherical grains, the growth of which is controlled by diffusion and by first-order and second-order crystal-growth kinetics as derived by Kahlweit (1975) (labeled curves). Also shown is the size distribution of chromite grains in samples D and E recalculated from area size distribution to volume size distribution and plotted as gray (sample D) and black (sample E) squares. Grain size, L, is normalized to mean grain size, $L_{average}$, whereas grain-size frequency, F, is normalized to the maximum value, $F_{most\ frequent}$.

nally derived independently by Lifshitz and Slyozov (1961) and by Wagner (1961) for diffusion-controlled growth and growth controlled by first-order reaction kinetics, and the work of these authors is now known as LSW theory. The LSW expressions have been extended to second-order reaction kinetics by Hanitzsch and Kahlweit (1969a, 1969b) and Kahlweit (1975), among others [a summary of these and other variations of LSW expressions is presented by Tsumuray and Miyata (1983) and Joesten (1991)]. In general, the theoretical CSD curves show only modest variations as a function of, for example, the volume fraction of solid phase or convection in the liquid, but the curves may broaden for solid phases with shapes that deviate significantly from the spherical assumption of LSW theory or if there is relative motion of grains and matrix (e.g., Hardy and Voorhees 1988).

Figure 5 shows curves predicted by LSW theory for three growth mechanisms, as well as the data from samples D and E. The CSD trends are approximated by the curve expected for a mineral if growth is controlled by second-order growth kinetics during aging, but they have much longer tails at the larger grain sizes, a feature also observed for olivine in mantle xenoliths (Jung et al. 1992). Also, the chromite CSD trends are wider than any of the predicted curves, as was also observed by Cashman and Ferry (1988) in their study of metamorphic mineral CSDs. In most cases the theoretical curves assume static temperature conditions, whereas in nature different times of entrapment of chromite grains during crystallization of the interstitial liquid would cause some areas to experience longer periods of aging in a partially liquid environment. The theoretical curves also typically assume grains are not locally impinging, that there is no growth by means other than by competitive grain growth, and that aging is spatially uniform with no region of the grain growing at the expense of other regions. As shown below, these last two assumptions of LSW theory are not likely to be true in the natural system and may be the cause of the differences between observed and predicted LSW trends.

For mineral aging in a closed system with no nucleation of new crystals, volume balance requires that the total number of grains present at any time be inversely proportional to the cube of the average crystal radius, or,

$$\frac{N_{total}(0)}{N_{total}(t)} = \left[\frac{\bar{r}(t)}{\bar{r}(0)}\right]^3 \quad (3)$$

where $N_{total}(0)$ and $N_{total}(t)$ are the total number of grains per unit volume at times 0 and t, respectively, and $\bar{r}(0)$ and $\bar{r}(t)$ are the average radius at times 0 and t, respectively. Following Cashman and Ferry (1988), one can assume, as a first approximation, that the original size distribution at $t = 0$ was equal to the log-linear trend extended throughout a sample's size range. For the log-linear correlation, the relationship between grain size and number density is

$$n = n_0 e^{-bL} \quad (4)$$

where n_0 is the intercept at $L = 0$ (as noted previously), and b is the slope of the linear portion of the trend. Integration of this expression with respect to L gives the total number of crystals at $t = 0$ (equivalent to the zero moment of the distribution):

$$N_{total}(0) = \int_0^\infty n_0 e^{-bL}\, dL = \frac{n_0}{b}. \quad (5)$$

Similarly, the total length of all crystals is given by integrating the number density over the length interval (equivalent to the first moment of the distribution):

$$L_{total} = \int_0^\infty L n_0 e^{-bL}\, dL = \frac{n_0}{b^2}. \quad (6)$$

Combining Equations 5 and 6 allows one to determine the average grain size, $\bar{L}$, and average crystal radius, $\bar{r}$:

$$2\bar{r} = \bar{L} = \frac{L_{total}}{N_{total}} = \frac{1}{b}. \quad (7)$$

Results for samples D, E, and F, and a comparison with the same calculation for the metapelite garnet sample of Cashman and Ferry (1988) shown in Figure 4, are presented in Table 1. Although the metamorphic garnet CSD curves tend to agree relatively well with the expected closed-system volume balance as expressed by Equation 3, the apparent volume of crystals in the cumulus chromite samples is in excess of three times larger than would be expected if aging occurred in a system closed to material influx.

The assumption that aging involved largely the loss of small crystals such that the linear portion of the CSD trends was not changed with time, implicit in the volume-balance calculation used above, is not strictly correct. That is, it assumes that smaller grains are lost without growth of larger grains and hence underestimates the vol-

TABLE 1. Comparison of average crystal size and total number of grains in original and annealed CSD for chromite

Sample	$\bar{r}(t)$*	$\bar{r}(0)$	$N_{total}(t)$	$N_{total}(0)$	$\frac{N_{total}(0)}{N_{total}(t)}$	$\left[\frac{\bar{r}(t)}{\bar{r}(0)}\right]^3$	$\left\{\frac{\left[\frac{\bar{r}(t)}{\bar{r}(0)}\right]^3}{\frac{N_{total}(0)}{N_{total}(t)}}\right\}$
D	0.0591	0.0248	12108	45307	3.74	13.5	3.62
E	0.0443	0.0236	7955	16910	2.13	6.7	3.13
F**							
(a) All	0.0504	0.0177	32502	161833	4.98	23.1	4.64
(b) Center	0.0667	0.0253	22772	102526	4.50	18.3	4.07
(c) Margin	0.0467	0.0142	39784	235118	5.91	35.8	6.06
711A†	0.0224	0.0047	470	37000	78.7	106.2	1.35

* Average sizes and total number density at time t are as measured from the sample; calculated original average size and total number density at $t = 0$ were calculated from the linear fit to the log-linear portion of the CSD trend.

** CSD data for sample F were collected from (a) all grains in the layer, (b) grains in the central one-third of the layer, and (c) grains in the marginal two-thirds of the layer.

† Sample 711A is from the CSD for the garnet in a metapelite shown in the inset in Figure 3 (from Cashman and Ferry 1988).

ume change during crystal aging; the increases in volume over time listed in Table 1 would be minimum estimates. As noted by Marsh and Ramini (1995), linear CSD trends would show a counterclockwise rotation during a period of crystal aging as large grains continue to grow at a faster rate than small grains, even if nucleation is still occurring. This can be tested using the data from the symmetrically size-graded layer shown in Figure 1. In this case, the counterclockwise rotation of the log-linear trend of the coarse-grained center relative to the finer-grained margins is in the proper sense for an aging assemblage. This also suggests that the lack of smaller sizes is indeed due to aging and is not caused by the cessation of nucleation late in the crystallization history by some other mechanism.

Following a volume-balance argument similar to the above, we can compare the observed volume of material in the center of the layer at time t but with the assumption that the original CSD at $t = 0$ was equal to the log-linear trend of the grains in the margins of the layer. In this case the mass-volume estimates also illustrate that the central part of the layer was far from closed and instead has considerably more crystalline material than do the margins:

$$\frac{\left[\frac{\bar{r}(t)}{\bar{r}(0)}\right]^3}{\frac{N_{total}(0)}{N_{total}(t)}} = 10.6. \quad (8)$$

Both methods of volume balance suggest an increase in volume relative to number density over time and imply that chromite components were continually added during the textural evolution of the rock. The most straightforward explanation is that chromite components were added from the magma in the chamber during aging without the nucleation of additional grains. This would require that the chromite remain in contact with the supernatant magma for a period of time equivalent to the typical residence (growth) time for chromite noted above (in excess of 5 yr). During this time the growing chromitite could not be isolated from the overlying liquid by crystallization of new, chromite-free cumulates above the growing layer.

Another explanation for the increase in volume during crystal aging is suggested by the interpretation of Boudreau (1994, 1995). It was shown that fine-scale layering, as exemplified by thin chromite seams, can be modeled as the result of (or at least enhanced by) crystal aging that occurs preferentially between regions rather than homogeneously throughout an assemblage. In this interpretation minor spatial variations in average grain size can lead to growth of larger, more favored grains at the expense of regions of smaller grains such that an assemblage with local minor textural variations in average grain size evolves, over time, a macroscopic pattern defined by regions that are either crystal rich or crystal poor. This model is based on a series of experimental observations that mineral segregation and pattern formation (as exemplified by the formation of Liesegang banding in precipitating salt solutions) may occur after the nucleation event and that crystal growth is largely the product of competitive growth during crystal aging (e.g., Feinn et al. 1978; Kai et al. 1982; Feeney et al. 1983). The competitive particle growth model for pattern formation in single-crystal systems was investigated by P. Ortoleva and coworkers in a series of studies (e.g., Feinn et al. 1978; Feeney et al. 1983).

The symmetrically size-graded layer in Figure 1 is consistent with a spatially nonuniform crystal-aging event such that larger grains in the center preferentially grow at the expense of smaller grains in the margins. In this case, growth of grains in the center of the layer would involve preferential migration of material from the margins, and thus the volume of material in the center would be greater than that in the margins, assuming both regions started out with equal volumes. A comparison of the observed volume of chromite per unit volume in the center with that in the margins is consistent with this interpretation:

$$\frac{\left[\frac{\bar{r}_{\text{center}}(t)}{\bar{r}_{\text{margin}}(t)}\right]^3}{\frac{N_{\text{total margin}}(t)}{N_{\text{total center}}(t)}} = 1.67. \quad (9)$$

The increase in volume of crystalline material over time, observed in all samples, would be consistent with dissolution of chromite originally present outside the current boundaries of the chromitite layers. This is supported by the occasional presence of very small chromite grains away from the chromitite layers, which we interpret as the few remaining grains from an initially more numerous population.

Conclusions

These results demonstrate that CSDs of cumulus minerals, although superficially similar to those of settled mineral grains in clastic sedimentary rocks, can be produced by in situ crystallization processes without crystal settling. They do not prove that crystal settling did not occur. However, the results of this study suggest that initial size distributions, however produced, were significantly modified during an aging event. In addition, the crystallization model discussed above suggests a natural continuum of crystallization processes as one goes from a quickly cooled environment such as a lava lake or small intrusion to a large layered intrusion such as the Stillwater Complex, with some predictable consequences.

If the above conclusions are accepted, then this study places some new constraints on models for chromitite formation. First, the log-linear leg of the CSD curves suggests that in situ nucleation and growth progressed without significant addition by crystal settling. This implies that local Cr concentrations in the liquid were high enough to cause the initial nucleation and growth of the original chromite populations without crystal settling, or that the initial nucleation and growth phase was the result of a continuous component flux to sites of crystal growth. Given the low Cr concentrations in silicate liquids and the extremely specific circumstances by which chromite could nucleate alone in large intrusions (e.g., Lipin 1992; Campbell and Murck 1993), it is more likely that Cr migrated to areas of crystal growth. This initial assemblage was then subsequently modified and volumetrically enhanced by favored growth of regions of larger crystal size by a later crystal-aging event. Although beyond the scope of this paper, we believe that any description of the origin of chromitites must include a complete accounting of interstitial silicate liquid and volatile fluid migration during compaction of and convection within the crystal pile, and possible liquid-fluid-solid reactions that can accompany such migrations (e.g., Meurer and Boudreau 1996; Nicholson and Mathez 1991).

The similarity between the grain-size histograms presented here and those of Jackson (1961) suggests that the results of this study are applicable to Ultramafic series chromitites. Grain-size histograms for plagioclase and pyroxene from the Lower Banded series (Page and Moring 1990) and for olivine from the Ultramafic series (Jackson 1961) also are similar to chromite CSDs. This suggests that most common minerals in layered intrusions had a similar crystallization history.

Parallels with CSD curves from metapelites suggest that log-linear trends overturned at smaller grain sizes should be a characteristic feature of many rocks that have undergone nucleation, growth, and then aging of the crystal assemblage. In particular, it explains the textural similarity commonly observed between plutonic igneous and undeformed high-grade metamorphic rocks.

Acknowledgments

This work was completed by C.W. as part of an undergraduate senior thesis at Duke University. Additional support was provided by NSF grants EAR-9217664 and EAR-9417144 to A.E.B. Reviews by R.A. Wiebe, D. Snyder, B. Marsh, K. Cashman, and W.P. Meurer led to significant improvements in the manuscript and are very much appreciated.

References cited

Boudreau, A.E. (1994) Crystal aging in two component, two crystal systems. South African Journal of Geology, 97, 473–485.

———(1995) Crystal aging and the formation of fine-scale layering. Mineralogy and Petrology, 54, 55–69.

Campbell, I.H. (1978) Some problems with the cumulus theory. Lithos, 11, 311–323.

Campbell, I.H., and Murck, B.W. (1993) Petrology of the G and H chromitite zones in the Mountain View area of the Stillwater Complex, Montana. Journal of Petrology, 34, 291–316.

Cashman, K.V. (1990) Textural constraints on the kinetics of crystallization of igneous rocks. In Mineralogical Society of America Reviews in Mineralogy, 24, 259–314.

Cashman, K.V., and Ferry, J.M. (1988) Crystal size distributions (CSD) in rocks and the kinetics and dynamics of crystallization: III. Metamorphic crystallization. Contributions to Mineralogy and Petrology, 99, 401–415.

Cashman, K.V., and Marsh, B.D. (1988) Crystal size distributions (CSD) in rocks and the kinetics and dynamics of crystallization: II. Makaopuhi lava lake. Contributions to Mineralogy and Petrology, 99, 292–305.

Feeney, R., Schmidt, S.L., Stricholm, P., Chadam, J., and Ortoleva, P. (1983) Periodic precipitation and coarsening waves: Applications of the competitive particle growth model. Journal of Chemical Physics, 78, 1293–1311.

Feinn, D., Ortoleva, P., Scalf, W., and Wolff, M. (1978) Spontaneous pattern formation in precipitating systems. Journal of Chemical Physics, 69, 27–39.

Hanitzsch, E., and Kahlweit, M. (1969a) Zur Umlosung aufgadampfter metallkristalle, 2. Zeitschrift für Physikalische Chemie (Frankfurt am Main), 65, 290–305.

———(1969b) Ageing of precipitates. In Industrial Crystallization, Proceedings of a Symposium Presented by the Institute of Chemical Engineers, London, 130–141.

Hardy, S.C., and Vorhees, P.W. (1988) Ostwald ripening in a system with a high volume fraction of coarsening phase. Metallurgical Transactions, 19A, 2713–2720.

Hunter, R.H. (1986) Textural equilibrium in layered igneous rocks. In I. Parsons, Ed., Origins of igneous layering, p. 473–503. Reidel, Boston.

Jackson, E.D. (1961) Primary textures and mineral associations in the Ultramafic zone of the Stillwater Complex, Montana. U.S. Geological Survey Professional Paper 358.

Joesten, R.L. (1991) Kinetics of coarsening and diffusion-controlled mineral growth. In Mineralogical Society of America Reviews in Mineralogy, 26, 507–582.

Jung, H., Faul, U.H., and Waff, H.S. (1992) Crystal size distributions of upper mantle xenoliths and experimentally produced ultramafic partial melts. Eos, 73, 502.

Kahlweit, M. (1975) Ostwald ripening of precipitates. Advances in Colloid Interface Science, 5, 1–35.

Kai, S., Muller, S.C., and Ross, J. (1982) Measurements of temporal and spatial sequences on events in periodic precipitation processes. Journal of Chemical Physics, 76, 1392–1406.

Lifshitz, I.M., and Slyozov, V.V. (1961) The kinetics of precipitation from supersaturated solid solutions. Journal of Physical Chemistry of Solids, 19, 35–50.

Lipin, B.R. (1992) Pressure increases, the formation of chromite seams, and the development of the Ultramafic series in the Stillwater Complex, Montana. Journal of Petrology, 34, 955–976.

Marsh, B.D. (1988) Crystal size distribution (CSD) in rocks and the kinetics and dynamics of crystallization: I. Theory. Contributions to Mineralogy and Petrology, 99, 277–291.

Marsh, B.D., and Ramini, R. (1995) Pivot points in crystal size distributions and solidification fronts and textural development in igneous rocks. Eos, 76, S293.

McBirney, A.R., and Noyes, R.M. (1979) Crystallization and layering of the Skaergaard intrusion. Journal of Petrology, 20, 487–554.

McCallum, I.S., Raedeke, L.D., and Mathez, E.A. (1980) Investigations of the Stillwater Complex: Part I. Stratigraphy and structure of the Banded zone. American Journal of Science, 280A, 59–87.

Meurer, W.P., and Boudreau, A.E. (1996) Compaction of density stratified cumulates: Effect on trapped liquid distributions. Journal of Geology, 104, 115–120.

Nicholson, D.M., and Mathez, E.A. (1991) Petrogenesis of the Merensky Reef in the Rustenburg section of the Bushveld Complex. Contributions to Mineralogy and Petrology, 107, 293–309.

Ostwald, W. (1900) Über die vermeintliche isomeric des roten und gelben quecksilberoxyds un die oberflächenspannung fester körper. Zeitschrift für Physikalishe Chemie Stöchiometrie und Verwandtschaftslehre, 34, 495–503.

Page, N.J., and Moring, B.C. (1990) Petrology of the noritic and gabbronoritic rock below the J-M Reef in the Mountain View area, Stillwater Complex, Montana. U.S. Geological Survey Bulletin, 1674-C.

Raedeke, L.D., and McCallum, I.S. (1984) Investigations of the Stillwater Complex: Part II. Petrology and petrogenesis of the Ultramafic series. Journal of Petrology, 25, 395–420.

Todd, S.G., Keith, D.W., LeRoy, L.W., Schissel, D.J., Mann, E.L., and Irvine, T.N. (1982) The J-M platinum-palladium Reef of the Stillwater Complex, Montana: I. Stratigraphy and petrology. Economic Geology, 77, 1454–1480.

Tsumuray, K., and Miyata, Y. (1983) Coarsening models incorporating both diffusion geometry and volume fraction of particles. Acta Metallurgica, 31, 437–452.

Wagner, C. (1961) Theorie der Alterung von Niederschlägen durch Umlosen (Ostwald Reifung). Zeitschrift für Elektrochemie, 65, 581–591.

Manuscript received January 2, 1996
Manuscript accepted July 22, 1996